Uniform, Binary Functionalization of a Metal-Organic Framework Material

Kanchana P. Samarakoon,‡ Christopher S. Satterfield,‡ Mechelle C. McCoy, Daniel A. Pivaral-Urbina, Timur Islamoglu,§ Victor W. Day,† Tendai Gadzikwa*

Department of Chemistry, Kansas State University, Manhattan, Kansas 66506, USA

Supporting Information Placeholder

ABSTRACT: General routes to confined spaces of well-defined chemical composition and complex 3-dimensional structure have long been sought by materials chemists. Here, we introduce metal-organic framework (MOF) materials as an ideal scaffold upon which such organized complexity can be built. Employing an orthogonal coordination strategy, we constructed a large-pore MOF material with two different modifiable linkers in well-defined positions relative to each other. The *independent* and *quantitative* covalent grafting of two distinct chemical groups onto these differently reactive linkers yielded a uniformly bifunctionalized MOF material. Not only does this methodology offer an efficient route via which the properties of well-defined microporous materials can be fine-tuned, it also creates a solid-state platform for synthetically accessing constructs that better emulate the well-ordered intricacy of biological structures.

The precise arrangement of cooperating chemical functionalities within confined space is a powerful design motif in biological systems. The motif is responsible for the unmatched catalytic performances of enzymes, prompting a decades-long search for general methods to incorporate it into catalytic materials.[1–3] Unfortunately, the organization of complex chemical functionality in 3-dimensions remains a fundamental challenge in materials chemistry. In particular, it is the defining challenge of supramolecular catalysis,[3–7] a field that seeks to construct confined spaces that are (i) decorated with multiple cooperatively-acting functionalities, (ii) flexible, and (iii) identical.[4,8,9]

While supramolecular capsules can boast of uniform confined interiors, the incompatibility of flexibility and secondary functionality with their assembly has precluded the construction of supramolecular structures that incorporate all of the above-listed design elements. With pore sizes on the order of small-molecule diameters, and composed of organic linkers in precisely-defined locations, metal-organic framework (MOF) materials bear many similarities with the bio-inspired, discrete supramolecular structures that have been developed over the decades.[7,10–16] What sets them apart is that, while there are examples of internally functionalizing discrete assemblies,[17] the process of rationally evolving MOFs post-assembly is appreciably more facile.[18–21] As a result of their robust framework structure, MOF pores can be systematically decorated with a variety of chemical functionalities, including those that are flexible and/or capable of participating in supramolecular interactions.[22–29] The post-assembly introduction of *multiple* such functionalities further increases the chemical and 3-dimensional complexity of the cavities,[24,25,30–32] satisfying two of the three desired elements for bio-inspired confined spaces (vide supra).

It is the third condition, that of generating uniformly multifunctionalized cavities, that has challenged MOF chemists. Telfer and co-workers have reported a family of well-defined MOF materials, assembled with 3 different organic components, whose chemical pore environment can be modulated by choice of organic linker.[33,34] This system beautifully illustrates the potential of MOFs to generate well-defined, multi-component, confined spaces, but it is a unique example. A more general route to such materials would be the introduction of multiple chemical functionalities into MOF cavities post-assembly. However, all of the prior-referenced methods of doing so unavoidably result in multivariate MOFs, i.e. frameworks whose pores are not identically functionalized.[24,25,30–32] Nevertheless, the methods of post-synthesis functionalization employed by the groups of Cohen[30] and Rosi[31] do offer insight into a strategy which could lead to uniform multifunctionalization. Their approaches were to independently functionalize orthogonally reactive linkers that were non-uniformly dispersed throughout their MOF materials (Figure 1A). Had the modifiable linkers been regularly positioned, these orthogonal modification strategies would have yielded uniformly multifunctional frameworks (Figure 1B). In this report, we detail how such an end has been realized via the independent functionalization of a well-defined, mixed-linker MOF material.

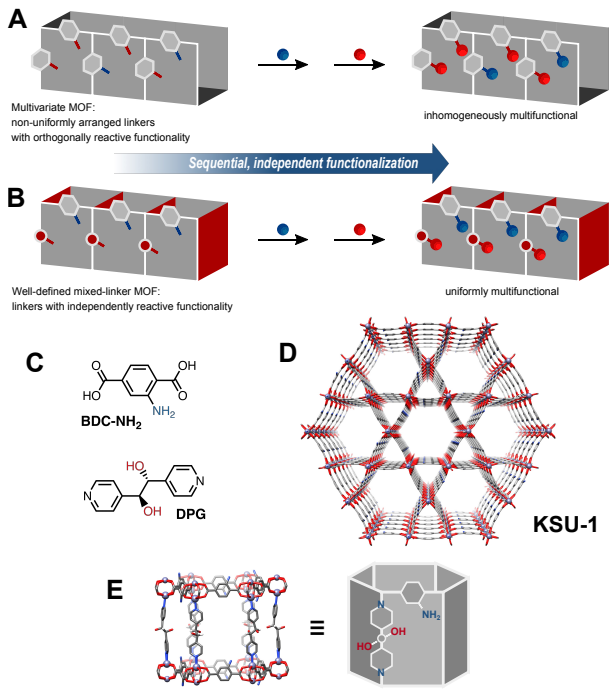

FIGURE 1. A: Independent functionalization of inhomogeneously dispersed, orthogonally reactive linkers in a MOF. B: Functionalization of independently reactive MOF linkers in well-defined locations resulting in a uniformly multifunctional MOF material. C: Independently modifiable MOF linkers with orthogonal coordination chemistry, **BDC-NH$_2$** and **DPG**. D: **KSU-1** framework viewed down the *c*-axis. E: Single network unit for **KSU-1** and its schematic representation.

Previous examples of independent multifunctionalization of MOFs involved linkers that were orthogonally modifiable, but which had identical coordination chemistry.[30,31] This resulted in materials in which the locations of these orthogonally reactive moieties were not well-defined (Figure 1A). Our strategy uses linkers that have independently reactive functional groups, *as well as* orthogonal coordination chemistries (Figure 1B). We opted for amines and hydroxyls as our reactive functionalities, and for carboxylates and pyridyls for the orthogonal coordination (Figure 1C). In combination with M^{2+} salts, dicarboxylates can form 2D nets with M^{2+}-paddlewheel secondary building units (SBUs), and these nets can be pillared by the dipyridyl linkers to yield mixed-linker structures with the different components in well-defined positions.[35] Although M^{2+}-paddlewheel MOFs typically form square nets, low temperature nucleation of the frameworks can afford the rarer Kagome-type lattices that have the large channels necessary for post-synthesis functionalization of MOFs.[36–38]

Gratifyingly, when 2-amino-1,4-benzenediacarboxylic acid (**BDC-NH$_2$**) and *meso*-*α*,*β*-di(4-pyrdyl)glycol (**DPG**) were incubated with $Zn(NO_3)_2{\cdot}6H_2O$ in DMF at 60 °C for two days, and then left at room temperature for another 2 days, a mixed-linker MOF material with a Kagome lattice (**KSU-1**) was obtained (Figure 1C-D). Single-crystal X-ray diffraction analysis of the resulting pale-yellow, block-like crystals revealed **BDC-NH$_2$** linkers connected by Zn-paddlewheel SBUs in the *ab*-plane, forming 2D sheets that are pillared together by **DPG** linkers along the *c*-axis (Figure 1D-E). The resulting structure has two channels along the *c*-axis: triangular and hexagonal channels that are 1 nm and 1.7 nm across, respectively. Powder X-ray diffraction (PXRD) analysis of **KSU-1** confirmed the purity of bulk phases of the material (Figure S1 in the Supporting Information [SI]), which was further corroborated by ^{1}H-NMR spectroscopy (Figure 2). Integration of the **BDC-NH$_2$** and **DPG** peaks indicated that the linkers were present in a 2:1 ratio respectively, which is as expected for a mixed-linker, paddle-wheel MOF (Figure S2, SI). Nitrogen adsorption isotherms at 77K of CO_2-activated **KSU-1** (Figure S3, SI) indicated that the material does not retain most of its porosity upon evacuation, however, thermogravimetric analysis (TGA, Figure S4, SI) confirmed that the material has significant solvent-accessible volume, with **KSU-1** losing ~50 % of its weight as DMF upon heating.

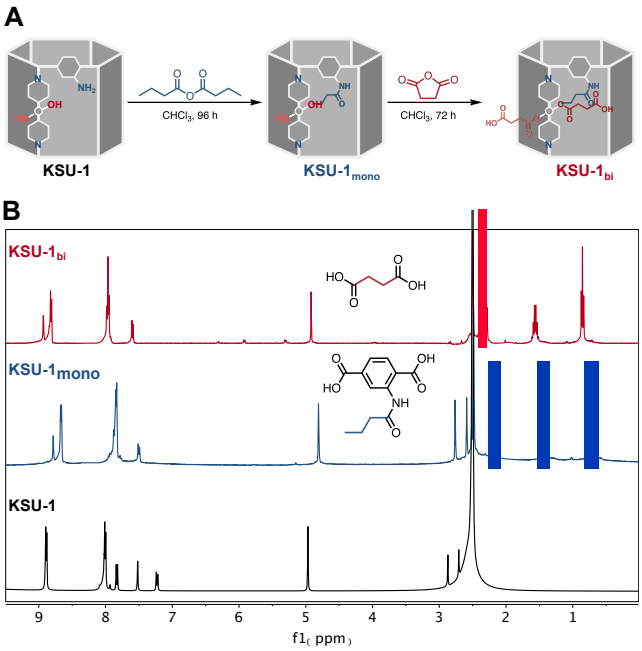

FIGURE 2. A: Schematic representation of sequential, independent functionalization of **KSU-1** with butyric anhydride followed by succinic anhydride. B: ^{1}H-NMR spectra of each material in the functionalization sequence digested in a solution of D_2SO_4 in d_6-DMSO. **KSU-1$_{mono}$**: new multiplets in the 0.5–2.30 ppm region correspond to the aliphatic butyryl chain protons. **KSU-1$_{bi}$**: the new singlet peak at 2.35 ppm corresponds to the aliphatic succinic acid protons. DMF is responsible for the peaks in the 2.60–2.90 ppm region.

Having established the purity and porosity of **KSU-1**, we proceeded to investigate post-synthesis modification. We hypothesized that the amine group of **BDC-NH$_2$** is sufficiently nucleophilic to react with linear aliphatic anhydrides under relatively low concentrations, while the hydroxyls of **DPG** is not. Butyric anhydride was chosen as the electrophile for the amidation reaction, which was performed following a modified literature procedure.[24] After immersing the MOF material in anhydrous $CHCl_3$ solutions of butyric anhydride for a total of 96 h, with constant agitation, the success of the reaction was evaluated using ^{1}H-NMR. The amidation product (**KSU-1$_{mono}$**) was thoroughly rinsed, evacuated, then digested in a solution of D_2SO_4 in d_6-DMSO. The ^{1}H-NMR spectrum obtained was compared to that of **KSU-1** (Figure 2B). All of the peaks corresponding to the parent **BDC-NH$_2$** protons had shifted, and new peaks which correspond to the protons of the butyryl substituent of the amide had appeared in the aliphatic region (0.5–2.5 ppm). The integration ratios were consistent with a **DPG**:butyryl ratio of 1:2, as expected for quantitative, and selective, functionalization of the amine (Figure S2, SI). Additionally, high-resolution electrospray ionization mass spectrometry (ESI-MS) of the MOF material digested in a solution of diazabicyclo[2.2.2]octane (DABCO) in DMSO revealed masses corresponding to **BDC-amide** and unreacted **DPG** only (Figure 3 and Figure S5, SI). Control experiments showed that the DABCO solution does not hydrolyze any esters present (*vide infra*), so this result further confirmed that the linear anhydride did not react with **DPG**.[39]

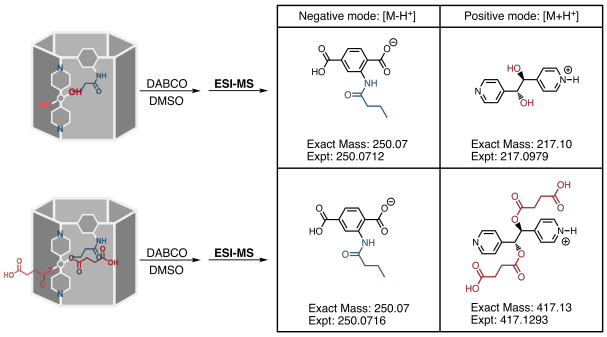

FIGURE 3. A: Schematic representation of the high resolution ESI-MS analysis of **KSU-1$_{mono}$** and **KSU-1$_{bi}$**. The **BDC** derivatives are ionized only in the negative mode, while the **DPG** derivatives are ionized only in the positive

mode. The spectra are available in the Supporting Information (Figure S5, SI. **KSU-1$_{mono}$**): in the negative mode, the [M-H$^+$] peak corresponds to deprotonated **BDC-amide**, while the [M+H$^+$] peak corresponds to protonated **DPG**. **KSU-1$_{bi}$**: in the negative mode, the [M-H$^+$] peak again corresponds to deprotonated **BDC-amide**, while the [M+H$^+$] peak corresponds to protonated **DPG-diester**.

The PXRD (Figure S1, SI) and TGA (Figure S4, SI) of **KSU-1$_{mono}$** indicated that the material retained its crystallinity and preserved significant porosity, with the material losing ~35 % of its weight as DMF. Adsorption isotherms with N_2 at 77K revealed that the porosity of evacuated **KSU-1$_{mono}$** could be accessed partially with CO_2 activation (Figure S3, SI). The large solvent-accessible volume that still remained in **KSU-1$_{mono}$** indicated that the second functionalization of the MOF material was feasible. We attempted the nucleophilic ring-opening of succinic anhydride by the **DPG** linker of **KSU-1$_{mono}$** to produce an aliphatic acid attached to **DPG** via an ester linkage, a reaction previously used for the monofunctionalization of a MOF material.[26] The MOF was immersed in a suspension of succinic anhydride in anhydrous $CHCl_3$ and agitated for 72 h to produce the bifunctionalized material **KSU-1$_{bi}$**. After washing and evacuation, **KSU-1$_{bi}$** was digested in a solution of D_2SO_4 in d_6-DMSO for ^{1}H-NMR analysis. Because of the acidic NMR solvent mixture, we expected that the labile ester linkage would be hydrolyzed and that the spectrum of **KSU-1$_{bi}$** would be identical to that of **KSU-1$_{mono}$**, except for the presence of aliphatic protons corresponding to the freed succinic acid. The results matched this scenario, with proton peak integration indicating a 1:1 ratio of succinic acid to butyric amide (Figure S3, SI). Since the –NH_2 to –OH ratio in the parent material **KSU-1** is also 1:1, this final result indicated the quantitative, independent functionalization of the **BDC-NH$_2$** and **DPG** linkers.

To confirm that the succinic acid was indeed covalently attached to the **DPG** via an ester linkage, **KSU-1$_{bi}$** was disassembled in a solution of DABCO in d_6-DMSO. Two separate signals corresponding to the –CH_2 protons of the ester derivative were present in the ^{1}H-NMR spectrum (Figure S2, SI), and a mass signal corresponding to the **DPG-diester** was present in the ESI-MS spectrum (Figure 3 and Figure S5, SI). Signals corresponding to unreacted **DPG** and **DPG-monoester** were not observed, further substantiating quantitative conversion. The PXRD pattern (Figure S1, SI) indicates that the material remained crystalline. Gas adsorption isotherms again revealed partial porosity (Figure S2, SI), as well as the presence of mesopores. These are attributed to the slight dissolution of linkers during the reactions. The TGA (Figure S4, SI) indicates that **KSU-1$_{bi}$** still has a large amount of solvent-accessible volume as it loses ~25% of its weight as DMF.

The ^{1}H-NMR and mass spectra support that the butyryl group is attached to **BDC-NH$_2$** while the succinic acid is tethered to **DPG**, thus we can conclude that these moieties are regularly arranged throughout the material. We should note that the –NH_2 group has positional disorder in the crystal. So, while the functionalization is regular in that each unit cell has the same components, their spatial arrangement is not identical.

In conclusion, we have taken two strategies for increasing the chemical diversity of MOF cavities – pillared mixed-linker MOF assembly and post-synthesis functionalization – and combined them to demonstrate a methodology for uniformly tailoring MOF pores with multiple functionalities. This new tool in the MOF construction arsenal opens exciting opportunities in the development of multifunctional MOFs. While the lack of permanent microporosity will limit this particular material and its multifunctionalized derivatives to solution-phase applications such as catalysis, the methodology we have demonstrated can serve as a blueprint as we seek to construct more robust materials. In this work, we modified the MOF with proof-of-concept moieties. However, one can envision employing this strategy to functionalize MOF cavities to achieve a myriad of cooperative actions in catalysis, detection, sequestration, etc. The uniformity of the strategy will increase the selectivity of these various applications and bring us closer to a long-standing goal of materials chemistry: the construction of highly functionalized, uniform, confined spaces in which the sophisticated functions of biological structures can be emulated.

ASSOCIATED CONTENT

Supporting Information. The Supporting Information is available free of charge on the ACS Publications website. Experimental details (PDF) and Crystallographic Information File (CIF).

AUTHOR INFORMATION

Corresponding Author

*gadzikwa@ksu.edu

Present Addresses

§ Department of Chemistry, Northwestern University, 2145 Sheridan Road, Evanston, Illinois 60208, United States
† X-Ray Crystallography Lab, University of Kansas, Lawrence, Kansas, 66045, USA.

Author Contributions

‡Authors contributed equally.

Funding Sources

This research was partially supported by National Science Foundation grant (CHE-9712735), as well as an NSF-MRI grant (CHE-0923449) to the University of Kansas that purchased the X-ray diffractometer and software used in this study.

ACKNOWLEDGMENT

The authors acknowledge Kansas State University for a College of Arts & Sciences Scholarship and an Office of Undergraduate Research & Creative Inquiry Grant for MCM, and for support from the Developing Scholars Program for DAP. The authors also acknowledge the Aakeröy Lab at K-State and the Farha Lab at Northwestern University for use of their equipment.

ABBREVIATIONS

BDC-NH_2, 2-amino-1,4-benzenediacarboxylic acid; DPG, *meso*-α,β-di(4-pyrdyl)glycol; SBU, secondary building unit.

REFERENCES

(1) Yu, C.; He, J. Synergic Catalytic Effects in Confined Spaces. *Chem. Commun.* **2012**, *48*, 4933–4940.
(2) Zhang, Y.; Li, B.; Ma, S. Dual Functionalization of Porous Aromatic Frameworks as a New Platform for Heterogeneous Cascade Catalysis. *Chem. Commun.* **2014**, *50*, 8507–8510.
(3) Mouarrawis, V.; Plessius, R.; van der Vlugt, J. I.; Reek, J. N. H. Confinement Effects in Catalysis Using Well-Defined Materials and Cages. *Front. Chem.* **2018**, *6*.
(4) Sanders, J. K. M. Supramolecular Catalysis in Transition. *Chem. – Eur. J.* **1998**, *4*, 1378–1383.
(5) Wulff, G. Enzyme-like Catalysis by Molecularly Imprinted Polymers. *Chem. Rev.* **2002**, *102*, 1–28.
(6) Dong, Z.; Luo, Q.; Liu, J. Artificial Enzymes Based on Supramolecular Scaffolds. *Chem. Soc. Rev.* **2012**, *41*, 7890–7908.
(7) Kuah, E.; Toh, S.; Yee, J.; Ma, Q.; Gao, Z. Enzyme Mimics: Advances and Applications. *Chem. – Eur. J.* **2016**, *22*, 8404–8430.
(8) Kirby, A. J. Enzyme Mechanisms, Models, and Mimics. *Angew. Chem. Int. Ed. Engl.* **1996**, *35*, 706–724.
(9) Hedstrom, L. Enzyme Specificity and Selectivity. In *eLS*; John Wiley & Sons, Ltd, 2001.
(10) Raynal, M.; Ballester, P.; Vidal-Ferran, A.; Leeuwen, P. W. N. M. van. Supramolecular Catalysis. Part 2: Artificial Enzyme Mimics. *Chem. Soc. Rev.* **2014**, *43*, 1734–1787.
(11) Zarra, S.; Wood, D. M.; Roberts, D. A.; Nitschke, J. R. Molecular Containers in Complex Chemical Systems. *Chem. Soc. Rev.* **2014**, *44*, 419–432.
(12) Deraedt, C.; Astruc, D. Supramolecular Nanoreactors for Catalysis. *Coord. Chem. Rev.* **2016**, *324*, 106–122.
(13) Otte, M. Size-Selective Molecular Flasks. *ACS Catal.* **2016**, *6*, 6491–6510.
(14) Guy, L.; Dutasta, J.-P.; Martinez, A. Endohedral Functionalization of Molecular Cavities for Catalysis in Confined Spaces. In *Effects of Nanoconfinement on Catalysis*; Poli, R., Ed.; Fundamental and Applied Catalysis; Springer International Publishing: Cham, 2017; pp 1–15.
(15) Yang, J.; Chatelet, B.; Hérault, D.; Dutasta, J.-P.; Martinez, A. Covalent Cages with Inwardly Directed Reactive Centers as Confined Metal and Organocatalysts. *Eur. J. Org. Chem.* **2018**, *2018*, 5618–5628.
(16) Holloway, L. R.; Bogie, P. M.; Lyon, Y.; Ngai, C.; Miller, T. F.; Julian, R. R.; Hooley, R. J. Tandem Reactivity of a Self-Assembled Cage Catalyst with Endohedral Acid Groups. *J. Am. Chem. Soc.* **2018**, *140*, 8078–8081.
(17) Roberts, D. A.; Pilgrim, B. S.; Nitschke, J. R. Covalent Post-Assembly Modification in Metallosupramolecular Chemistry. *Chem. Soc. Rev.* **2018**, *47*, 626–644.
(18) Islamoglu, T.; Goswami, S.; Li, Z.; Howarth, A. J.; Farha, O. K.; Hupp, J. T. Postsynthetic Tuning of Metal–Organic Frameworks for Targeted Applications. *Acc. Chem. Res.* **2017**, *50*, 805–813.
(19) Cohen, S. M. The Postsynthetic Renaissance in Porous Solids. *J. Am. Chem. Soc.* **2017**, *139*, 2855–2863.
(20) Bosch, M.; Yuan, S.; Rutledge, W.; Zhou, H.-C. Stepwise Synthesis of Metal–Organic Frameworks. *Acc. Chem. Res.* **2017**, *50*, 857–865.
(21) Yin, Z.; Wan, S.; Yang, J.; Kurmoo, M.; Zeng, M.-H. Recent Advances in Post-Synthetic Modification of Metal–Organic Frameworks: New Types and Tandem Reactions. *Coord. Chem. Rev.* **2017**.
(22) J. Ingleson, M.; Barrio, J. P.; Guilbaud, J.-B.; Z. Khimyak, Y.; J. Rosseinsky, M. Framework Functionalisation Triggers Metal Complex Binding. *Chem. Commun.* **2008**, *0*, 2680–2682.
(23) Doonan, C. J.; Morris, W.; Furukawa, H.; Yaghi, O. M. Isoreticular Metalation of Metal−Organic Frameworks. *J. Am. Chem. Soc.* **2009**, *131*, 9492–9493.
(24) Garibay, S. J.; Wang, Z.; Tanabe, K. K.; Cohen, S. M. Postsynthetic Modification: A Versatile Approach Toward Multifunctional Metal-Organic Frameworks. *Inorg. Chem.* **2009**, *48*, 7341–7349.
(25) Liu, H.; Xi, F.-G.; Sun, W.; Yang, N.-N.; Gao, E.-Q. Amino- and Sulfo-Bifunctionalized Metal–Organic Frameworks: One-Pot Tandem Catalysis and the Catalytic Sites. *Inorg. Chem.* **2016**, *55*, 5753–5755.
(26) Gadzikwa, T.; Farha, O. K.; Mulfort, K. L.; Hupp, J. T.; Nguyen, S. T. A Zn-Based, Pillared Paddlewheel MOF Containing Free Carboxylic Acids via Covalent Post-Synthesis Elaboration. *Chem. Commun.* **2009**, *0*, 3720–3722.
(27) Gee, W. J.; Cadman, L. K.; Amer Hamzah, H.; Mahon, M. F.; Raithby, P. R.; Burrows, A. D. Furnishing Amine-Functionalized Metal–Organic Frameworks with the β-Amidoketone Group by Postsynthetic Modification. *Inorg. Chem.* **2016**, *55*, 10839–10842.

(28) Kronast, A.; Eckstein, S.; Altenbuchner, P. T.; Hindelang, K.; Vagin, S. I.; Rieger, B. Gated Channels and Selectivity Tuning of CO2 over N2 Sorption by Post-Synthetic Modification of a UiO-66-Type Metal–Organic Framework. *Chem. – Eur. J.* **2016**, *22*, 12800–12807.
(29) Fracaroli, A. M.; Siman, P.; Nagib, D. A.; Suzuki, M.; Furukawa, H.; Toste, F. D.; Yaghi, O. M. Seven Post-Synthetic Covalent Reactions in Tandem Leading to Enzyme-like Complexity within Metal–Organic Framework Crystals. *J. Am. Chem. Soc.* **2016**, *138*, 8352–8355.
(30) Kim, M.; Cahill, J. F.; Prather, K. A.; Cohen, S. M. Postsynthetic Modification at Orthogonal Reactive Sites on Mixed, Bifunctional Metal–Organic Frameworks. *Chem. Commun.* **2011**, *47*, 7629–7631.
(31) Liu, C.; Luo, T.-Y.; Feura, E. S.; Zhang, C.; Rosi, N. L. Orthogonal Ternary Functionalization of a Mesoporous Metal–Organic Framework via Sequential Postsynthetic Ligand Exchange. *J. Am. Chem. Soc.* **2015**, *137*, 10508–10511.
(32) Keenan, L. L.; Hamzah, H. A.; Mahon, M. F.; Warren, M. R.; Burrows, A. D. Secondary Amine-Functionalised Metal–Organic Frameworks: Direct Syntheses versus Tandem Post-Synthetic Modifications. *CrystEngComm* **2016**, *18*, 5710–5717.
(33) Liu, L.; Zhou, T.-Y.; Telfer, S. G. Modulating the Performance of an Asymmetric Organocatalyst by Tuning Its Spatial Environment in a Metal–Organic Framework. *J. Am. Chem. Soc.* **2017**, *139*, 13936–13943.
(34) Zhou, T.-Y.; Auer, B.; Lee, S. J.; Telfer, S. G. Catalysts Confined in Programmed Framework Pores Enable New Transformations and Tune Reaction Efficiency and Selectivity. *J. Am. Chem. Soc.* **2019**, *141*, 1577–1582.
(35) Ma, B.-Q.; Mulfort, K. L.; Hupp, J. T. Microporous Pillared Paddle-Wheel Frameworks Based on Mixed-Ligand Coordination of Zinc Ions. *Inorg. Chem.* **2005**, *44*, 4912–4914.
(36) Chun, H.; Moon, J. Discovery, Synthesis, and Characterization of an Isomeric Coordination Polymer with Pillared Kagome Net Topology. *Inorg. Chem.* **2007**, *46*, 4371–4373.
(37) Kondo, M.; Takashima, Y.; Seo, J.; Kitagawa, S.; Furukawa, S. Control over the Nucleation Process Determines the Framework Topology of Porous Coordination Polymers. *CrystEngComm* **2010**, *12*, 2350–2353.
(38) Zhou, K.; Chaemchuen, S.; Wu, Z.; Verpoort, F. Rapid Room Temperature Synthesis Forming Pillared Metal-Organic Frameworks with Kagomé Net Topology. *Microporous Mesoporous Mater.* **2017**, *239*, 28–33.
(39) Madrahimov, S. T.; Atesin, T. A.; Karagiaridi, O.; Sarjeant, A. A.; Farha, O. K.; Hupp, J. T.; Nguyen, S. T. Metal–Organic Frameworks Containing (Alkynyl)Gold Functionalities: A Comparative Evaluation of Solvent-Assisted Linker Exchange, de Novo Synthesis, and Post-Synthesis Modification. *Cryst. Growth Des.* **2014**, *14*, 6320–6324.

The uniform, covalent post-synthesis bifunctionalization of a metal-organic framework (MOF) material is reported for the first time. A large-pore MOF material composed of two linkers that have orthogonal coordination chemistry and that bear independently reactive functional groups has been constructed. The subsequent covalent grafting of two different chemical functionalities onto these reactive linkers is both independent and quantitative, yielding uniformly bifunctionalized confined spaces.